Appl. Math. Mech. -Engl. Ed., **32**(4), 459–468 (2011)
DOI 10.1007/s10483-011-1430-6

Applied Mathematics and Mechanics (English Edition)

Analytical solutions for transverse distributions of stream-wise velocity in turbulent flow in rectangular channel with partial vegetation*

Wen-xin HUAI (槐文信), Chuan GENG (耿　川), Yu-hong ZENG (曾玉红), Zhong-hua YANG (杨中华)

(State Key Laboratory of Water Resources and Hydropower Engineering Science, Wuhan University, Wuhan 430072, P. R. China)

Abstract The theory of poroelasticity is introduced to study the hydraulic properties of the steady uniform turbulent flow in a partially vegetated rectangular channel. Plants are assumed as immovable media. The resistance caused by vegetation is expressed by the theory of poroelasticity. Considering the influence of a secondary flow, the momentum equation can be simplified. The momentum equation is nondimensionalized to obtain a smooth solution for the lateral distribution of the longitudinal velocity. To verify the model, an acoustic Doppler velocimeter (ADV) is used to measure the velocity field in a rectangular open channel partially with emergent artificial rigid vegetation. Comparisons between the measured data and the computed results show that the method can predict the transverse distributions of stream-wise velocities in turbulent flows in a rectangular channel with partial vegetation.

Key words theory of poroelasticity, open channel flow, vegetation, secondary current, depth-averaged velocity distribution

Chinese Library Classification TV131.2
2010 Mathematics Subject Classification 76F99

1 Introduction

Vegetation, such as trees, grass, and bushes, always grows in channels, rivers, and wetlands. Vegetation can increase the resistance and reduce the velocity in flows, which has a negative influence on the flood control. However, the vegetation in flows can promote the sediment deposition, reduce the river bed erosion, improve the environment of water, and restore the river ecological systems. Therefore, it is important to study the influences of vegetation on flows.

During the past decades, researchers have focused on the resistance of vegetation to flows and established some empirical relationships between vegetation and flows[1–2]. With the development of measure equipments, many researchers, e.g., Bennett et al.[3], Liu and Shen[4], Shimizu et al.[5], Stone and Shen[6], Tsujimoto and Kitamura[7], Wang et al.[8], Wu et al.[9], and Yang et al.[10], were more interested in the distributions of the velocity and the Reynolds stress.

* Received Sept. 29, 2010 / Revised Mar. 8, 2011
Project supported by the National Natural Science Foundation of China (Nos. 10972163 and 51079102) and the Fundamental Research Funds for the Central Universities (No. 2104001)
Corresponding author Wen-xin HUAI, Professor, Ph. D., E-mail: wxhuai@whu.edu.cn

At the same time, researchers became interested in the flows in partially vegetated channels, and obtained numerous experiment results about the vegetated channel flows. Based on the Shiono and Knight model (SKM)[11], Huai et al.[12], Rameshwaran and Shiono[13], and Tang and Knight[14] provided a 2-D analytical solution of a depth averaged stream-wise velocity for straight over bank flows in the compound channels with vegetation floodplains.

Recently, Hsieh and Shiu[15] introduced the theory of poroelasticity to the study of water flows passing over a vegetal area, mainly for getting the 2-D analytical solutions in the vertical velocity profile for the water flow passing over a vegetal area. The advantages of this method are that the vegetation area is regarded as homogeneous and isotropic porous media, and the results are accurate. The momentum equations of the flow in a vegetation area are given based on Biot's theory of poroelasticity[16].

We introduce the theory of poroelasticity to analysis the hydraulic properties of the turbulent flow in partially vegetated rectangular channels, which will provide a new type of expressions of the vegetation drag force. The Reynolds averaged Navier-Stokes (RANS) equation is integrated over the depth so as to solve the stream-wise velocity. To avoid the disadvantages of the dimensional express, e.g., the parameters appeared in the solutions are too large, this paper introduces a dimensionless control equation. By integrating and solving the equation, we acquire a new method to predict the depth-averaged velocity. Comparisons between our experimental data and the related data from Tsujimoto and Kitamura[7] show that our solutions behave effectively in predicting the transverse distributions of the depth averaged velocity.

2 Mathematical models

The turbulent flow in partially vegetated rectangular channels can be divided into two subregions along the transverse direction, i.e., the vegetated region and the non-vegetated region. According to Hsieh and Shiu[15], the momentum equation of the flow passing over a vegetal area is

$$\begin{aligned}&\alpha\rho\frac{\partial\overline{u}_i}{\partial t}+\alpha\rho\frac{\partial(\overline{u}_i\overline{u}_j)}{\partial x_j}\\&=-\frac{\mu\alpha^2}{k}\overline{u}_i+\rho g_i-\alpha\frac{\partial\overline{p}}{\partial x_i}+\mu\frac{\partial^2\overline{u}_i}{\partial x_j^2}+\alpha\frac{\partial}{\partial x_j}(-\rho\overline{u_i'u_j'}),\end{aligned}\tag{1}$$

where $x_i=(x,y,z)$ is the direction tensor, in which x, y, and z are the longitudinal, transverse, and vertical directions as shown in Fig. 1. $\overline{u}_i=(\overline{u}_x,\overline{u}_y,\overline{u}_z)$ is the velocity tensor, $\overline{u}_x$, $\overline{u}_y$, and $\overline{u}_z$ are the temporal mean velocities along the x-, y-, and z-directions, respectively. g_i is the

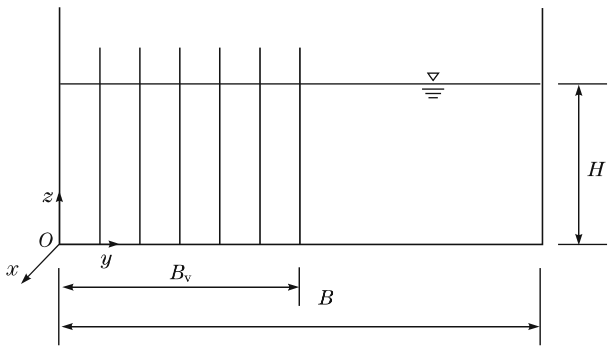

Fig. 1 Sketch of partially vegetated channel

gravitational acceleration tensor. $u_i' = (u_x', u_y', u_z')$ is the velocity fluctuation tensor, u_x', u_y', and u_z' are the velocity fluctuations along the x-, y-, and z-directions, respectively. The porosity α is defined as

$$\alpha = 1 - N_{\rm v} A_{\rm v},$$

where $A_{\rm v} = \frac{1}{4}\pi D^2$ is the cross-sectional area of a single stick[13]. $N_{\rm v}$ is the number of the sticks in a unit area. D is the diameter of a single stick. ρ is the water density. $-\frac{\mu\alpha^2}{k}\overline{u}_i$ is the expression of the vegetation resistance according to the theory of poroelasticity. μ is the water viscosity. k is the special permeability of the porous media.

From Eq. (1), we obtain the momentum equation along the x-direction in the steady uniform turbulence flow,

$$\alpha\rho\Big(\frac{\partial(\overline{u}_x\overline{u}_y)}{\partial y} + \frac{\partial(\overline{u}_x\overline{u}_z)}{\partial z}\Big) = \alpha\rho g S_0 + \alpha\frac{\partial\overline{\tau}_{yx}}{\partial y} + \alpha\frac{\partial\overline{\tau}_{zx}}{\partial z} - \frac{\mu\alpha^2}{k}\overline{u}_x, \tag{2}$$

where g is the gravitational acceleration. S_0 is the energy slope, which is equal to the bottom slope in the uniform flow. Since $\mu\frac{\partial^2\overline{u}_i}{\partial x_j^2}$ can be ignored in turbulence flows, the Reynolds stresses are as follows:

$$\begin{cases} \overline{\tau}_{yx} = -\rho\overline{u_y' u_x'}, \\ \overline{\tau}_{zx} = -\rho\overline{u_z' u_x'}. \end{cases}$$

Ervine et al.[17] assumed that the secondary flows were related to inertia as they did in their quasi-2D models,

$$\overline{u}_x\overline{u}_y = LU^2, \tag{3}$$

where U was the depth averaged stream-wise velocity, i.e.,

$$U = \frac{1}{H}\int_0^H \overline{u}_x {\rm d}z,$$

and L was the secondary current intensity coefficient, which was assumed to be constant in a specific case. The value of L will increase when the secondary current becomes more intense. Integrating Eq. (2) over the flow depth, we obtain the depth-averaged equation

$$\alpha\rho H L\frac{\partial U^2}{\partial y} + \alpha\rho\int_0^H {\rm d}(\overline{u}_x\overline{u}_z) = \alpha\rho g H S_0 + \alpha\int_0^H \frac{\partial\overline{\tau}_{yx}}{\partial y}{\rm d}z + \alpha\int_0^H {\rm d}\overline{\tau}_{zx} - \int_0^H \frac{\mu\alpha^2}{k}\overline{u}_x{\rm d}z. \tag{4}$$

The vertical velocity is usually zero at both the bed and the water surfaces, i.e.,

$$\overline{u}_z = 0 \quad \text{when} \quad z = 0 \quad \text{and} \quad z = H.$$

Thus, the second term in Eq. (4) is zero, i.e.,

$$\alpha\rho\int_0^H \mathrm{d}(\overline{u}_x\overline{u}_z)=0.$$

The Reynolds stress can be dealt with as follows:

$$\overline{\tau}_{yx}=\rho\overline{v}_t\frac{\mathrm{d}U}{\mathrm{d}y}, \tag{5}$$

where $\overline{v}_t$ is the depth-averaged eddy viscosity,

$$\overline{v}_t=\xi HU_*=\xi HU\sqrt{\frac{f}{8}}$$

with the eddy viscosity coefficient ξ and the Darcy-Weisbach friction factor f. Therefore,

$$\int_0^H \frac{\partial\overline{\tau}_{yx}}{\partial y}\mathrm{d}z=\rho\xi H^2\sqrt{\frac{f}{8}}\frac{\mathrm{d}}{\mathrm{d}y}\Big(U\frac{\mathrm{d}U}{\mathrm{d}y}\Big). \tag{6}$$

Meanwhile, assuming that $\overline{\tau}_{zx}$ at the water surface is zero, we have

$$\int_0^H \mathrm{d}\overline{\tau}_{zx}=-\tau_b, \tag{7}$$

where τ_b is the bed shear stress decided by

$$\tau_b=\frac{\rho fU^2}{8}.$$

Thus, Eq. (4) becomes

$$\rho gHS_0+\frac{\mathrm{d}}{\mathrm{d}y}\Big(\rho\xi H^2\sqrt{\frac{f}{8}}U\frac{\mathrm{d}U}{\mathrm{d}y}-\rho HLU^2\Big) -\frac{1}{8}\rho fU^2-\frac{\mu\alpha}{k}U=0. \tag{8}$$

It is very hard to get the analytical solution to Eq. (8). Thus, to get the analytical solution, we assume

$$\frac{\mu\alpha}{k}U=\frac{\mu\alpha}{k\overline{U}}U^2,$$

where $\overline{U}$ is the average velocity over the cross section of the vegetated area. Then, Eq. (8) is changed to

$$\rho gHS_0+\frac{\mathrm{d}}{\mathrm{d}y}\Big(\rho\xi H^2\sqrt{\frac{f}{8}}U\frac{\mathrm{d}U}{\mathrm{d}y}-\rho HLU^2\Big) -\frac{1}{8}\rho fU^2-\frac{\mu\alpha}{k\overline{U}}U^2=0. \tag{9}$$

Since there is no vegetation in the non-vegetated region, the control equation in this area is

$$\rho gHS_0+\frac{\mathrm{d}}{\mathrm{d}y}\Big(\rho\xi H^2\sqrt{\frac{f}{8}}U\frac{\mathrm{d}U}{\mathrm{d}y}-\rho HLU^2\Big) -\frac{1}{8}\rho fU^2=0. \tag{10}$$

Some researchers, e.g., Abril and Knight[18], Ervine et al.[17], and Huai et al.[12], have presented analytical solutions for predicting the transverse distribution of velocities. However, since the unknown constants in the solution are dimensional, the physical meaning of the solution is not clear. The relative parameters sometimes are too large, which makes the calculating results inaccurate. To overcome this shortage, this paper converts Eqs. (9) and (10) into the dimensionless form with the parameters as follows:

$$Y = \frac{y}{B}, \tag{11}$$

$$\eta = \frac{8U^2}{\alpha g H S_0 \sqrt{8f}}. \tag{12}$$

Dividing Eqs. (9) and (10) by

$$\frac{\alpha g H S_0 f}{8B^2},$$

we have

$$\frac{\mathrm{d}^2\eta}{\mathrm{d}Y^2} + A_{\mathrm{v}}\frac{\mathrm{d}\eta}{\mathrm{d}Y} + C_{\mathrm{v}}\eta + D_{\mathrm{v}} = 0 \quad \text{(in the vegetated region)}, \tag{13}$$

$$\frac{\mathrm{d}^2\eta}{\mathrm{d}Y^2} + A_{\mathrm{nv}}\frac{\mathrm{d}\eta}{\mathrm{d}Y} + C_{\mathrm{nv}}\eta + D_{\mathrm{nv}} = 0 \quad \text{(in the non-vegetated region)}, \tag{14}$$

where the subscripts v and nv represent the vegetated region and the non-vegetated region, respectively, and

$$\begin{cases} A_{\mathrm{v}} = -\dfrac{2BK}{\xi_{\mathrm{v}} H\sqrt{\dfrac{f_{\mathrm{v}}}{8}}}, \quad C_{\mathrm{v}} = -\dfrac{2B^2}{\xi_{\mathrm{v}} H^2\sqrt{\dfrac{f_{\mathrm{v}}}{8}}}\Big(\dfrac{f_{\mathrm{v}}}{8} + \dfrac{\mu\alpha}{k\overline{U}\rho}\Big), \\ D_{\mathrm{v}} = \dfrac{16B^2}{f_{\mathrm{v}} H^2 \xi_{\mathrm{v}}}, \quad A_{\mathrm{nv}} = -\dfrac{2BK}{\xi_{\mathrm{nv}} H\sqrt{\dfrac{f_{\mathrm{nv}}}{8}}}, \\ C_{\mathrm{nv}} = -\dfrac{2B^2}{\xi_{\mathrm{nv}} H^2}\sqrt{\dfrac{f_{\mathrm{nv}}}{8}}, \quad D_{\mathrm{nv}} = \dfrac{16B^2}{f_{\mathrm{nv}} H^2 \xi_{\mathrm{nv}}}. \end{cases}$$

Then, the dimensionless parameter η can be solved from Eqs. (13) and (14), i.e.,

$$\eta = I_1 \mathrm{e}^{r_1 Y} + I_2 \mathrm{e}^{r_2 Y} + \delta_{\mathrm{v}} \quad \text{(in the vegetated region)}, \tag{15}$$

$$\eta = I_3 \mathrm{e}^{r_3 Y} + I_4 \mathrm{e}^{r_4 Y} + \delta_{\mathrm{nv}} \quad \text{(in the non-vegetated region)}, \tag{16}$$

where I_i $(i = 1, 2, 3, 4)$ are the dimensionless unknown constants. How to decide I_i with the boundary conditions will be introduced in the next section. Other parameters in Eqs. (15) and (16) are

$$\begin{cases} \delta_{\mathrm{v}} = -\dfrac{D_{\mathrm{v}}}{C_{\mathrm{v}}}, \quad r_{1,2} = \dfrac{-A_{\mathrm{v}} \pm \sqrt{A_{\mathrm{v}} - 4C_{\mathrm{v}}}}{2}, \\ \delta_{\mathrm{nv}} = -\dfrac{D_{\mathrm{nv}}}{C_{\mathrm{nv}}}, \quad r_{3,4} = \dfrac{-A_{\mathrm{nv}} \pm \sqrt{A_{\mathrm{nv}} - 4C_{\mathrm{nv}}}}{2}. \end{cases}$$

From Eqs. (15) and (16), we can acquire the analytic solutions to Eqs. (9) and (10), i.e.,

$$U=\Big(\alpha\sqrt{\frac{f_{\rm v}}{8}}gHS_0(I_1{\rm e}^{r_1Y}+I_2{\rm e}^{r_2Y}+\delta_{\rm v})\Big)^{\frac{1}{2}}\quad \text{(in the vegetated region)},\tag{17}$$

$$U=\Big(\alpha\sqrt{\frac{f_{\rm nv}}{8}}gHS_0(I_3{\rm e}^{r_3Y}+I_4{\rm e}^{r_4Y}+\delta_{\rm nv})\Big)^{\frac{1}{2}}\quad \text{(in the non-vegetated region)}.\tag{18}$$

3 Estimation of parameters and progress of obtaining accurate results

The special permeability of the porous media is calculated by the Kozeny-Carman formula

$$k=\frac{c_0T\alpha^3}{(1-\alpha)^2M^2},$$

where c_0 is the Kozeny constant, which is 0.5 in a circular section and 0.667 in a long strip section, respectively. We adopt $c_0=0.667$ in this study. T is the tortuosity of porous media, whose value is 0.5 as suggested by Carman. M is the specific surface area, which is defined as the ratio of the surface area to the solid volume. The stronger the plants system is, the greater the value of M is. Here, $M=5.0\times10^3$ is adopted.

The boundary conditions to determine the unknown constants I_1, I_2, I_3, and I_4 are as follows:

(a) The velocity is zero at the edges of the channel, i.e.,

$$\begin{cases}U(Y=0)=0,\\ U(Y=1)=0.\end{cases}$$

(b) The velocity and its gradient are continuous at the interface of the two regions, i.e.,

$$\begin{cases}U\Big(Y=\dfrac{B_{\rm v}^-}{B}\Big)=U\Big(Y=\dfrac{B_{\rm v}^+}{B}\Big),\\ \dfrac{{\rm d}U}{{\rm d}Y}\Big|_{Y=\frac{B_{\rm v}^-}{B}}=\dfrac{{\rm d}U}{{\rm d}Y}\Big|_{Y=\frac{B_{\rm v}^+}{B}},\end{cases}$$

where $B_{\rm v}$ is the width of the vegetated region.

As a result, the unknown constants can be solved from the following matrix:

$$\begin{pmatrix}1&1&0&0\\0&0&{\rm e}^{r_3}&{\rm e}^{r_4}\\ \sqrt{f_{\rm v}}{\rm e}^{r_1\frac{B_{\rm v}}{B}}&\sqrt{f_{\rm v}}{\rm e}^{r_2\frac{B_{\rm v}}{B}}&-\sqrt{f_{\rm nv}}_2{\rm e}^{r_3\frac{B_{\rm v}}{B}}&-\sqrt{f_{\rm nv}}{\rm e}^{r_4\frac{B_{\rm v}}{B}}\\ \sqrt{f_{\rm v}}{\rm r}_1{\rm e}^{r_1\frac{B_{\rm v}}{B}}&\sqrt{f_{\rm v}}{\rm r}_2{\rm e}^{r_2\frac{B_{\rm v}}{B}}&-\sqrt{f_{\rm nv}}{\rm r}_3{\rm e}^{r_3\frac{B_{\rm v}}{B}}&-\sqrt{f_{\rm nv}}{\rm r}_4{\rm e}^{r_4\frac{B_{\rm v}}{B}}\end{pmatrix}\begin{pmatrix}I_1\\I_2\\I_3\\I_4\end{pmatrix}$$

$$=\begin{pmatrix}-\delta_{\rm v}\\-\delta_{\rm nv}\\ \sqrt{f_{\rm nv}}\delta_{\rm nv}-\sqrt{f_{\rm v}}\delta_{\rm v}\\0\end{pmatrix}.$$

The expressions of I_1, I_2, I_3, and I_4 are

$$\begin{cases} I_1 = -\delta_{\rm v} - I_2, \quad I_3 = -\dfrac{\delta_{\rm nv} + {\rm e}^{r_4} I_4}{{\rm e}^{r_3}}, \\ I_2 = \dfrac{G + \sqrt{f_{\rm nv}}{\rm e}^{r_3 \frac{B_{\rm v}}{B}} I_3 + \sqrt{f_{\rm nv}}{\rm e}^{r_4 \frac{B_{\rm v}}{B}} I_4}{\sqrt{f_{\rm v}}({\rm e}^{r_4 \frac{B_{\rm v}}{B}} - {\rm e}^{r_3 \frac{B_{\rm v}}{B}})}, \\ I_4 = \dfrac{mG - N\delta_{\rm nv} - \sqrt{f_{\rm v}} r_1 {\rm e}^{r_1 \frac{B_{\rm v}}{B}} \delta_{\rm v}}{\sqrt{f_{\rm nv}} r_4 {\rm e}^{r_4 \frac{B_{\rm v}}{B}} - m\sqrt{f_{\rm nv}}{\rm e}^{r_4 \frac{B_{\rm v}}{B}} + N{\rm e}^{r_4}}, \end{cases}$$

where

$$\begin{cases} G = \sqrt{f_{\rm nv}}\delta_{\rm nv} + \sqrt{f_{\rm v}}{\rm e}^{r_1 \frac{B_{\rm v}}{B}} \delta_{\rm v} - \sqrt{f_{\rm v}}\delta_{\rm v}, \\ m = \dfrac{r_4 {\rm e}^{r_4 \frac{B_{\rm v}}{B}} - r_3 {\rm e}^{r_3 \frac{B_{\rm v}}{B}}}{{\rm e}^{r_4 \frac{B_{\rm v}}{B}} - {\rm e}^{r_3 \frac{B_{\rm v}}{B}}}, \\ N = \dfrac{m\sqrt{f_{\rm nv}} r_3 {\rm e}^{r_3 \frac{B_{\rm v}}{B}} - \sqrt{f_{\rm nv}} r_3 {\rm e}^{r_3 \frac{B_{\rm v}}{B}}}{{\rm e}^{r_3}}. \end{cases}$$

The Darcy-Weisbach friction factors $f_{\rm v}$ and $f_{\rm nv}$ in the matrix above are decided by the Manning equation in the rectangle channel, i.e.,

$$f_{\rm v} = 8\frac{g n_{\rm v}^2}{R_{\rm v}^{\frac{1}{3}}}, \tag{19}$$

$$f_{\rm nv} = 8\frac{g n_{\rm nv}^2}{R_{\rm nv}^{\frac{1}{3}}}, \tag{20}$$

where $n_{\rm v}$ is the Manning coefficient in the vegetated region, while $n_{\rm nv}$ is the Manning coefficient in the non-vegetated region. $R_{\rm v}$ and $R_{\rm nv}$ are the hydraulic radii in the vegetated and non-vegetated regions, respectively. The detailed method to decide the friction factors can be found in [12].

The eddy viscosity coefficient in the non-vegetated region $\xi_{\rm nv}$ is supposed to be constant, i.e., $\xi_{\rm nv} = 0.07$[18]. We suppose that the Reynolds stress is continuous at the interface of the regions as follows:

$$\overline{\tau}_{yx}\Big(\frac{B_{\rm v}^-}{B}\Big) = \overline{\tau}_{yx}\Big(\frac{B_{\rm v}^+}{B}\Big), \tag{21}$$

$$\begin{aligned} \overline{\tau}_{yx} &= \rho\overline{\upsilon}_t \frac{{\rm d}U}{{\rm d}y} \\ &= \frac{\rho f_{\rm v}}{16}\alpha\xi_{\rm v} g H S_0 (I_1 r_1 {\rm e}^{r_1 Y} + I_2 r_2 {\rm e}^{r_2 Y})\frac{H}{B} \quad \text{(in the vegetated region)}, \end{aligned} \tag{22}$$

$$\begin{aligned} \overline{\tau}_{yx} &= \rho\overline{\upsilon}_t \frac{{\rm d}U}{{\rm d}y} \\ &= \frac{\rho f_{\rm nv}}{16}\alpha\xi_{\rm nv} g H S_0 (I_3 r_3 {\rm e}^{r_3 Y} + I_4 r_4 {\rm e}^{r_4 Y})\frac{H}{B} \quad \text{(in the non-vegetated region)}. \end{aligned} \tag{23}$$

Then, the eddy viscosity coefficient in the vegetated region $\xi_{\rm v}$ can be estimated by

$$\xi_{\rm v} = \sqrt{\frac{f_{\rm nv}}{f_{\rm v}}}\xi_{\rm nv}. \tag{24}$$

Though the secondary flow will decrease in the vegetated region owing to the resistance of vegetation, the second current intensity coefficient L is still considered. L is related to a variety of factors such as the channel shape, the roughness coefficient, the flow depth, the vegetation density, etc. Referring to the value range suggested by Ervine et al.[17] (L is about 0.5% for straight channels), the try-out method is used to estimate the value of L.

With the relative parameters given above, we can get the first-step calculated depth-averaged velocities U. However, the results are not accurate because of the assumption that

$$\frac{\mu\alpha}{k}U = \frac{\mu\alpha}{k\overline{U}}U^2.$$

To improve the results, we use the first-step results to get the value of $C_{\mathrm{v}2}$ calculated by

$$C_{\mathrm{v}2} = -\frac{2B^2}{\xi_{\mathrm{v}} H^2\sqrt{\frac{f_{\mathrm{v}}}{8}}}\Big(\frac{f_{\mathrm{v}}}{8} + \frac{\mu\alpha}{kU\rho}\Big).$$

Then, the obtained $C_{\mathrm{v}2}$ is substituted for C_{v} in the expression of

$$\delta_{\mathrm{v}} = -\frac{D_{\mathrm{v}}}{C_{\mathrm{v}}}.$$

Therefore, δ_{v}, r_1, and r_2 become variable. The expressions of the boundary conditions and the equation-solved matrix are the same as before except that the values of δ_{v}, r_1, and r_2 should be the values at the place of

$$Y = \frac{B_{\mathrm{v}}}{B}.$$

Then, we can get a new series of U by solving the equation-solved matrix so as to get the respective parameters.

We circulate the progress above until the results of two continuous steps are almost the same, and the accurate convergency (the difference of the results between the final two steps is less than 0.1%) is reached.

4 Experiments and results

The experiments are conducted in a straight rectangular glass flume with the length of 20 m, the width of 0.5 m, and the depth of 0.44 m. The bed slope S_0 is set to be 0.04%. The steel bars are used to simulate the rigid vegetation, and the mean velocities are measured by an ADV system. The flow discharge is controlled by an electric magnetic valve, and the water surface is adjusted to be about 0.04% by the gate installing at the end of the flume. All experiments are carried out under the uniform conditions. The vegetation is emergent in the two cases shown in Table 1. To validate the applicability of the calculated results, the experimental parameters of other researchers are also listed in Table 1.

Table 1 Parameters of laboratory experiments

Source	Case	Flume width B/m	Vegetated area B_{v}/m	Water depth width H/m	Porosity α/m	Energy slope S_0/%
Our experiments	1	0.5	0.250	0.110 0	0.992 1	0.040
	2	0.5	0.250	0.180 0	0.996 1	0.040
Tsujimoto and Kitamura[7]	A	0.4	0.120	0.050 0	0.992 0	0.165
	B	0.4	0.120	0.045 7	0.991 6	0.170

Figures 2–5 show the comparisons between the experimental data and the calculated results. From the figures, we can see that the predicted depth-averaged velocities agree well with the measured data when the secondary current intensity coefficient L has an optimum value. Moreover, the values of L have the same order as the magnitude.

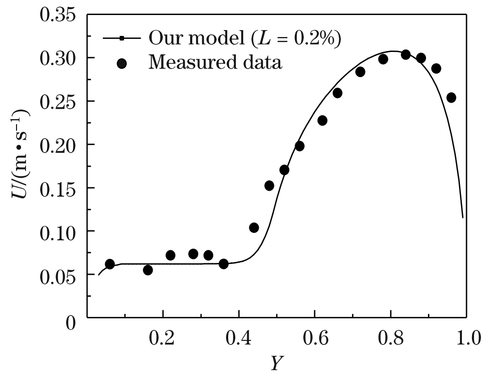

Fig. 2 Comparison of our predicted U with our experimental data in Case 1

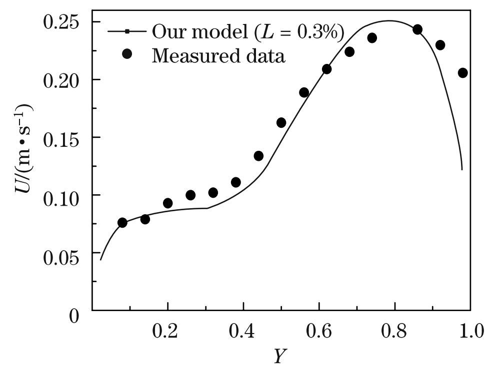

Fig. 3 Comparison of our predicted U with our experimental data in Case 2

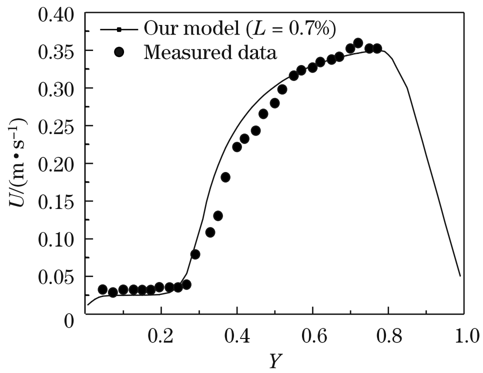

Fig. 4 Comparison of our predicted U with Tsujimoto and Kitamura's experimental data[7] in Case A

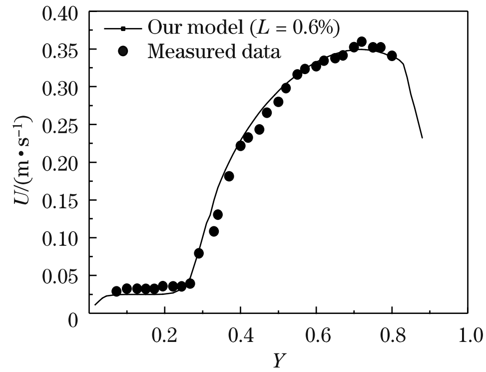

Fig. 5 Comparison of our predicted U with Tsujimoto and Kitamura's experimental data[7] in Case B

5 Conclusions

This paper establishes the momentum equations in both vegetated and non-vegetated regions after considering the effects of the secondary current and resistance of vegetation, and converts them into a dimensionless form. The resistance caused by vegetation is expressed by the theory of poroelasticity. After determining the boundary conditions and solving the equations, a method is established to predicate the depth-averaged velocity of a steady uniform flow with the emergent rigid vegetation partially planted in rectangular channels. An ADV is used to measure the velocity for the partially vegetated rectangular channel. Comparisons between the calculated results and the experimental data show that our proposed method can provide an effective prediction for the depth-averaged velocity. Comparisons between different runs of the calculated results show that the values of the secondary current intensity have the same order as the magnitude under different flow conditions.

References

[1] Cowna, W. L. Estimating hydraulic roughness coefficients. *Agriculture Engineering*, **37**(7), 473–475 (1956)

[2] Kouwen, N. and Unny, T. E. Flexible roughness in open channels. *Journal of the Hydraulics Division*, **99**(5), 713–728 (1973)

[3] Bennett, S. J., Pirim, T., and Barkdoll, B. D. Using simulated emergent vegetation to alter stream flow direction within a straight experimental channel. *Geomorphology*, **44**(1-2), 115–126 (2002)

[4] Liu, C. and Shen, Y. M. Flow structure and sediment transport with impacts of aquatic vegetation. *Journal of Hydrodynamics*, *Series B*, **20**(4), 461–468 (2008)

[5] Shimizu, Y., Tsujimoto, T., Nakagawa, H., and Kitamura, T. Experimental study on flow over rigid vegetation simulated by cylinders with equi-spacing (in Japanese). *Proceedings of the Japan Society of Civil Engineers*, **438**, 31–40 (1991)

[6] Stone, B. M. and Shen, H. T. Hydraulic resistance of flow in channels with cylindrical roughness. *Journal of Hydraulic Engineering*, **128**(5), 500–506 (2002)

[7] Tsujimoto, T. and Kitamura, T. *Experimental Study on Open-Channel Flow with Vegetated Zone along Side Wall*, KHL Progressive Report, Hydraulic Laboratory, Kanazawa University, Japan, 21–35 (1992)

[8] Wang, C., Zhu, P., Wang, P. F., and Zhang, W. M. Effects of aquatic vegetation on flow in the Nansi Lake and its flow velocity modeling. *Journal of Hydrodynamics*, *Series B*, **18**(6), 640–648 (2006)

[9] Wu, F. C., Shen, H. W., and Chou, Y. J. Variation of roughness coefficients for unsubmerged and submerged vegetation. *Journal of Hydraulic Engineering*, **125**(9), 934–942 (1999)

[10] Yang, K. J., Liu, X. N., Cao, S. Y., and Zhang, Z. X. Turbulence characteristics of overbank flow in compound river channel with vegetated floodplain (in Chinese). *Journal of Hydraulic Engineering*, **36**(10), 1263–1268 (2005)

[11] Shiono, K. and Knight, D. W. Turbulent open channel flows with variable depth across the channel. *Journal of Fluid Mechanics*, **222**(5), 617–646 (1991)

[12] Huai, W. X., Gao, M., Zeng, Y. H., and Li, D. Two-dimensional analytical solution for compound channel flows with vegetated floodplains. *Applied Mathematics and Mechanics* (*English Edition*), **30**(9), 1121–1130 (2009) DOI 10.1007/s10483-009-0906-z

[13] Rameshwaran, P. and Shiono, K. Quasi two-dimensional model for straight overbank flows through emergent vegetation on floodplains. *Journal of Hydraulic Research*, **45**(3), 302–315 (2007)

[14] Tang, X. N. and Knight, D. W. Lateral distributions of streamwise velocity in compound channels with partially vegetated floodplains. *Science in China*, *Series E*: *Technological Sciences*, **52**(11), 3357–3362 (2009)

[15] Hsieh, P. C. and Shiu, Y. S. Analytical solutions for water flow passing over a vegetal area. *Advances in Water Resources*, **29**(9), 1257–1266 (2006)

[16] Biot, M. A. Theory of propagation of elastic waves in a fluid saturated porous solid, I: low-frequency range. *Journal of the Acoustical Society of America*, **28**(2), 168–178 (1956)

[17] Ervine, D. A., Babaeyan-Koopaei, K., and Sellin, R. H. J. Two-dimensional solution for straight and meandering overbank flows. *Journal of Hydraulic Engineering*, **126**(9), 653–669 (2000)

[18] Abril, J. B. and Knight, D. W. Stage-discharge prediction for rivers in flood applying a depth-averaged mode. *Journal of Hydraulic Research*, **42**(6), 616–629 (2004)